Liquid Crystals
Publication details, including instructions for authors and subscription information:
http://www.informaworld.com/smpp/title~content=t713926090

Ferrielectric smectic phases: Liquid crystal structure and macroscopic fluctuations

V. L. Lorman[a]
[a] Laboratoire de Physique de la Matière Condensée, Université de Picardie, Amiens Cedex, France

To cite this Article Lorman, V. L.(1996) 'Ferrielectric smectic phases: Liquid crystal structure and macroscopic fluctuations', Liquid Crystals, 20: 3, 267 — 276
To link to this Article: DOI: 10.1080/02678299608032034
URL: http://dx.doi.org/10.1080/02678299608032034

LIQUID CRYSTALS, 1996, VOL. 20, NO. 3, 267–276

Ferrielectric smectic phases: Liquid crystal structure and macroscopic fluctuations†

by V. L. LORMAN*

Laboratoire de Physique de la Matière Condensée, Université de Picardie, 33 rue Saint Leu, 80039 Amiens Cedex, France

(*Received 21 July 1995; accepted 26 September 1995*)

The work concerns the structures and properties of multilayer smectic phases with complex tilt and dipolar order. The symmetry and thermodynamical classification of multilayer antiferroelectric and ferrielectric phases is given. The main attention is paid to the difference of these phases with respect to classical ferroelectric S_C^*. A two-layer model of the ferrielectric smectic phase is generalized to describe the sequence of the first order phase transitions ferro–ferri–antiferro-electric and to show the possibility of existence of two isostructural ferrielectric phases, which differ in the value of the helical pitch and in the sense of the helix.

1. Introduction

In recent years, many experimental studies have been performed on liquid crystal compounds which show new types of smectic phases with complex tilt and dipolar order, namely antiferroelectric $S_{C_A}^*$ and ferrielectric $S_{C_\gamma}^*$ phases and a whole number of other sub-phases [1–8]. Initially, two-layer tilted phases were discovered in the 1980s [9–11], but the polymorphism of corresponding substances was not realized.

Although the sets of experiments on the new series of liquid crystals embraced X-ray diffraction [12, 13], differential scanning calorimetry (DSC) [5, 14, 15], helicoidal structure studies [1, 16], phason dispersion analysis [17] and conoscopic observations under an external electric field [6, 7, 18, 19], the structures of the reported phases are not yet clear. The X-ray studies on oriented plates show the absence of any detectable modulation of electronic density along the z axis, which suggests strongly that the tilt angle is identical from one layer to another. The layer spacing $d(T)$, as a function of temperature [12, 13, 20, 21], varies very slowly when crossing between S_C^*, $S_{C_\gamma}^*$ and $S_{C_A}^*$ phases with no qualitative difference between the X-ray diffraction images in these phases. Thus, only indirect methods of structure determination are available for the moment. One has to construct a limited number of realistic structural models to analyse and then to deduce their physical properties and verify experimentally the consequences.

In a series of studies [22–26], in order to explain the set of experimental data concerning phases with complex tilt and dipolar order, it is proposed that a bilayer periodicity for the smectic stacking is assumed. In our previous studies [25, 26], we have shown that the sequence of transitions involving ferro-, ferri- and anti-ferro-electric phases can be understood in terms of an azimuthal reorientation of the molecular sub-units in adjacent smectic layers. Some recent experimental data, especially conoscopic observations using an external electric field [18, 19, 27], have generated a number of structural models supposing the existence of three-, four- and even multilayered phases [see, for example, 4, 16] as the steps of a possible Devil's staircase. However, neither the symmetries of the structures nor symmetry restrictions on the parameters of the proposed structures have been analysed. In [28], a systematic symmetry and thermodynamical analysis of the possible antiferroelectric and ferrielectric structures induced by multilayer tilt ordering from a parent S_A phase has been performed, which has reduced significantly the choice of structural models. This work has revealed considerable difference in molecular organization of the multilayer tilted smectic phases with respect to the classical monolayer S_C^* phase, although it deals only with basic unwound structures of the phases.

In general, we can summarize several new unusual features of phases with complex tilt and dipolar ordering as follows:

(1) There can exist several ordered tilted phases with the same number of layers in the unit cell: (a) five antiferroelectric basic structures for each fixed value n of the number of layers ($n > 2$); (b) seven tilted structures for each fixed value of n ($n > 2$) in achiral substances, all of them of the 'antiferro'-

*Author for correspondence.
† Presented at the European Conference on Liquid Crystals, Bovec, Slovenia, March 1995.

type, i.e. the sum of the axial vectors characterizing tilts in n layers is equal to zero; (c) from (a) and (b) it follows that the basic unwound structures of the multilayer phases in chiral and achiral substances are rather different, which was not the case for S_C and S_C^* phases.

(2) All tilted antiferroelectric phases with $n > 2$ have an azimuthal angle between adjacent layers different from zero: $0 \neq \psi \neq \pi$. This means that the molecules in corresponding structures are not situated in the same plane, as was the case in S_C and S_C^* phases (and even in bilayer $S_{C_A}^*$ or S_O structures).

(3) Each basic unwound structure can generate several different inhomogeneous phases (helicoidal, modulated, doubly modulated, etc.). Furthermore, some of them can be stable only in an external electric field. Thus, it is practically impossible to obtain unequivocal information about basic unwound structures by studying the behaviour of the inhomogeneous phases in an external electric field.

(4) There can exist two different stable states with qualitatively the same helicoidal structure, but with a different elastic energy of the helix. Such kinds of structures can be called isostructural helicoidal phases.

(5) The transition between ferro- and antiferro-electric phases through an intermediate ferrielectric structure can reveal fluctuations of the molecules between two equivalent positions on the cone in the ferrielectric phase. This mechanism can lead on the macroscopic level to the breaking of continuity of the ferrielectric helicoidal structure with formation of multiple defects. Spontaneous switching of these defects should be seen as macroscopic fluctuations in all types of optical experiments. For each fixed value of temperature, the density of these defects has to be fixed and represents an intrinsic characteristic of the ferrielectric phase.

In the present work we focus our attention mainly on points (1a), (1c), (2) and (4) of this list. The remaining points are the subject of papers which will be published elsewhere.

The paper is organized as follows: in § 2, a theoretical analysis is presented of the possible molecular organization that may arise in multilayer antiferroelectric and ferrielectric smectics. Points (1a), (1c) and (2) of the above list are clarified. Realistic structures which can probably take part in the Devil's staircase sequence of phases are presented. It is shown that the mechanism of formation of the eventual Devil's staircase is the azimuthal reorientation of the molecules in neighbouring layers.

In § 3, the model of the two-layer ferrielectric phase [25, 26] is generalized to explain the actual order of the phase transitions ferro- ferri- and ferri- antiferroelectric and to show the possibility of existence of two isostructural ferrielectric phases of the $S_{C_\gamma}^*$-type (see also point (2) of the preceding list). It is shown that these two ferrielectric phases have no qualitative difference, but differ by the sense of their helices and by the absolute value of their helicoidal pitches. § 4 contains a brief discussion of the results obtained.

2. Multilayer antiferroelectric and ferrielectric structures

Let us perform the symmetry analysis of possible multilayer tilted phases in chiral smectics in two steps. *At the first step*, we will study all different *basic unwound structures* of the antiferroelectric type which can be obtained from the parent S_A phase by way of phase transition. To obtain *helicoidal* or other *inhomogeneous phases* which correspond to the basic structures one has to add *at the second step* the inhomogeneous term F_{inhom} to the Landau–de Gennes free energy of the S_A phase:

$$\Phi = (S/V) \int (F_{\text{hom}} + F_{\text{inhom}}) \mathrm{d}z. \qquad (1)$$

Here the sum extends over the thickness of the sample; S is its section area and V is its volume. F_{inhom} contains invariants which depend on the gradients of the order parameter (OP), while F_{hom} depends usually only on invariants which are polynomials in the function of *OP*. Then, classical Euler–Lagrange procedure gives the types of inhomogeneous structures and their domains of stability (see for example [23, 25] for the types and stability of the bilayer helicoidal structures).

The classification of the basic unwound structures of the tilted smectic phases is based on the classification of the irreducible representations of the space group of symmetry of the S_A phase. Such a method was first proposed by Indenbom *et al.* [29, 30] (see also [31]).

Let us introduce for the phenomenological description of the phases the axial vectors of the tilts defined as follows:

$$\boldsymbol{\eta}_i = (-n_{iy} n_{iz}, n_{ix} n_{iz}) \qquad (2)$$

where n_{iu} ($u = x, y, z$) are the components of the director in the ith layer and the space variables (x, y) and z are, respectively, the in-layer coordinates and the direction perpendicular to the smectic plane.

The components of the tilt axial vectors $\boldsymbol{\eta}_i$ span different representations of the space group G_o of the parent S_A phase. G_o contains the sub-group of discrete one-dimensional translations along the z axis T_z and the continuous sub-group of all the in-plane rotations and displacements. Note that in the case of achiral molecules, the point group of the smectic layer is $D_{\infty h}$, though in the chiral case, the inversion of the media is lost and the point group of the layer is D_{∞}.

The low-symmetry ordered tilted phases can be divided into *three* wide *classes* according to their translational periodicity, i.e. to the number of smectic layers in the unit cell. Actually, the one-dimensional Brillouin zone of the S_A phase has only two points with particular symmetry: (i) $\mathbf{k} = 0$ (the centre of the zone) and (ii) $\mathbf{k} = (1/2)c^*$ (its border), where $c^* = 2\pi/d$ and d is the interlayer distance, these particular points being connected by the line of equivalent points of general type (see figure 1). If the transition from the S_A phase leads to the phase in which one-layer periodicity is preserved, then the wave vector of the tilt ordering is associated with the centre of the zone (see figure 1 (*a*)). This is the case of a S_C phase in achiral substances and of a ferroelectric S_C^* phase in chiral materials. Analogously, all the bilayer tilted smectic phases correspond to the wave vector $\mathbf{k} = (1/2)c^*$ (see figure 1 (*b*)), associated with the border of the zone. This class of phases is larger than the previous one. It contains, for example, the S_O phase, i.e. a bilayer, herringbone-structured phase with achiral molecules. The antiferroelectric $S_{C_A}^*$ phase and three possible unwound, basic ferrielectric structures with bilayer periodicity [25] also belong to this class.

Let us now consider the case of the wave vector with the end lying inside the Brillouin zone, so that $\mathbf{k} = (1/n)c^*$, where $n > 2$ (see figure 1 (*c*)). The symmetry of all the wave vectors lying between $\mathbf{k} = 0$ and $\mathbf{k} = (1/2)c^*$ is exactly the same; consequently the length of the wave vector of the corresponding tilt ordering can vary continuously with temperature. This is the simple reason for the possibility of the so-called Devil's staircase, which

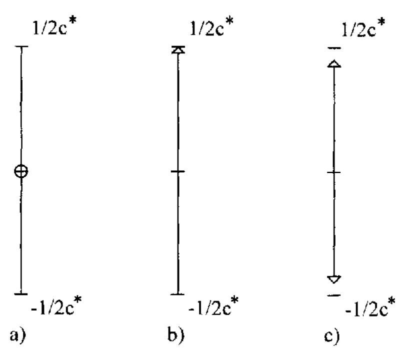

Figure 1. Different types of wave vector in the Brillouin zone of the S_A phase. (*a*) $\mathbf{k} = 0$ associated with the S_C^* phase; (*b*)a$\mathbf{k} = (1/2)c^*$ associated with the $S_{C_A}^*$ phase and two-layer ferrielectric phases; (*c*) $\mathbf{k} = (1/n)c^*$ associated with multilayer antiferroelectric phases.

can result in the existence of the succession of phases with different translational periodicity (different integral number of layers in the unit cell) connected by the regions of stability of the incommensurate phases [32, 33]. The purpose of this section is to give the classification of basic homogeneous unwound structures induced by the tilt ordering associated with this third type of wave vector. We will limit here our consideration to the case of chiral smectics in order to give a realistic description of the Devil's staircase which can eventually occur in chiral smectics, having both ferroelectric and antiferroelectric phases in their polymorphism.

To illustrate the structure of multilayer tilted smectic phases with n layers in the unit cell, let us take the example of $n = 4$. In this case, four successive layers are involved in the ordering. The phase transition from the S_A phase to the four-layer antiferroelectric phase is characterized by four axial vectors of tilt of the layers: $\boldsymbol{\eta}_1, \boldsymbol{\eta}_2, \boldsymbol{\eta}_3, \boldsymbol{\eta}_4$ defined as in equation (2). They form four symmetric axial vector combinations which can be considered as different axial vector order parameters (*OP*):

$$\left.\begin{aligned} \boldsymbol{\eta}_P &= \boldsymbol{\eta}_1 + \boldsymbol{\eta}_2 + \boldsymbol{\eta}_3 + \boldsymbol{\eta}_4, \\ \boldsymbol{\eta}_{A1} &= \boldsymbol{\eta}_1 + \boldsymbol{\eta}_2 - \boldsymbol{\eta}_3 - \boldsymbol{\eta}_4, \\ \boldsymbol{\eta}_{A2} &= \boldsymbol{\eta}_1 - \boldsymbol{\eta}_2 - \boldsymbol{\eta}_3 + \boldsymbol{\eta}_4, \\ \boldsymbol{\eta}_{A3} &= \boldsymbol{\eta}_1 - \boldsymbol{\eta}_2 + \boldsymbol{\eta}_3 - \boldsymbol{\eta}_4. \end{aligned}\right\}, \tag{3}$$

All the vectors in equation (3) are planar and have zero z-component. Only two of them, $\boldsymbol{\eta}_{A1}$ and $\boldsymbol{\eta}_{A2}$, are associated with the wave vector $\mathbf{k} = (1/4)c^*$ and can induce four-layer ordering. They transform in the same way as two different vectors of antipolarization $\mathbf{A}_1 = \mathbf{P}_1 + \mathbf{P}_2 - \mathbf{P}_3 - \mathbf{P}_4$ and $\mathbf{A}_2 = \mathbf{P}_1 - \mathbf{P}_2 - \mathbf{P}_3 + \mathbf{P}_4$ of the four-layer antiferroelectric structure and represent its essential characteristics. Here $\mathbf{P}_i$ is the polarization of the ith layer. Two remaining symmetric combinations in (3) cannot induce four-layer ordering, because they are associated with the wave vector that is different from $\mathbf{k} = (1/4)c^*$. The first axial vector $\boldsymbol{\eta}_P$ transforms in the same way as the macroscopic polarization $\mathbf{P} = \mathbf{P}_1 + \mathbf{P}_2 + \mathbf{P}_3 + \mathbf{P}_4$ and is associated with $\mathbf{k} = 0$. Such *OP* can lead only to a S_C^* phase in a chiral smectogen. The last axial vector $\boldsymbol{\eta}_{A3}$ is associated with $\mathbf{k} = (1/2)c^*$. It transforms as the bilayer polarization $\mathbf{A} = \mathbf{P}_1 - \mathbf{P}_2$ and can lead to a $S_{C_A}^*$ phase. Thus, $\boldsymbol{\eta}_P$ and $\boldsymbol{\eta}_{A3}$ are secondary *OP* of the four-layer ordering.

If we are interested only in four-layer ordering, we can put $\boldsymbol{\eta}_P$ and $\boldsymbol{\eta}_{A3}$ equal to zero. Then, it follows that in all antiferroelectric four-layer phases $\boldsymbol{\eta}_1 = -\boldsymbol{\eta}_3$ and $\boldsymbol{\eta}_2 = -\boldsymbol{\eta}_4$; the tilt of the first layer is always opposite to the tilt of the third, and the tilt of the second layer is always opposite to the tilt of the fourth. From the point of view of the spatial symmetry of the structure, this means that there exists a common symmetry element, which is preserved in all four-layer antiferroelectric structures. This element is the two-fold screw axis along the z-direction.

In order to describe all possible basic unwound structures of the four-layer tilt ordering, one has to look for the minima of the homogeneous part of the Landau–de Gennes free energy as a function of the components of the $\boldsymbol{\eta}_{A1}$ and $\boldsymbol{\eta}_{A2}$ axial vectors.

Note, that in chiral media, the symmetry of the S_A parent phase has no spatial inversion; the point group which preserves the wave vector $\mathbf{k}=(1/n)c^*$ $(n>2)$ is C_∞. Consequently, $\boldsymbol{\eta}_{A1}$ and $\boldsymbol{\eta}_{A2}$ span two irreducible representations of the S_A^* space group. That is, the x-component of $\boldsymbol{\eta}_{A1}$ and the y-component of $\boldsymbol{\eta}_{A2}$ form one OP and the x-component of $\boldsymbol{\eta}_{A2}$ and the y-component of $\boldsymbol{\eta}_{A1}$ form another OP. These two OP are always coupled, so that in the free energy there appears an invariant $I_D=[\boldsymbol{\eta}_{A1}\times\boldsymbol{\eta}_{A2}]$, the vector product of the planar vectors $\boldsymbol{\eta}_{A1}$ and $\boldsymbol{\eta}_{A2}$. This invariant is similar to those introduced by Dzyaloshinskii to explain the phenomenon of the weak ferromagnetism of antiferromagnetics [34]. In the theory of exchange magnetics, this invariant also appears in the case where the components of two magnetization vectors are mixed and distributed between two different representations of the paramagnetic phase. The value of I_D defines the angle between different sub-lattices; in our case it is the azimuthal angle between the tilt vectors of even and odd layers.

The homogeneous part of the Landau–de Gennes free energy of the 4-layer antiferroelectric ordering depends on three basic invariants:

$$F^*_{\mathrm{hom}}=F(I_1,I_2,I_3) \tag{4}$$

where $I_1=(\eta_{A1})^2+(\eta_{A2})^2$, $I_2=(\eta_{A1})^2(\eta_{A2})^2$ and $I_3=[\boldsymbol{\eta}_{A1}\times\boldsymbol{\eta}_{A2}]=\eta_{A1}\eta_{A2}\sin\alpha$. Possible low-symmetry phases are defined by minima of F^*_{hom}:

$$(\mathrm{d}F_{\mathrm{hom}}/\mathrm{d}\eta_i)=(\mathrm{d}F_{\mathrm{hom}}/\mathrm{d}I_m)(\mathrm{d}I_m/\mathrm{d}\eta_i)=0 \tag{5}$$

where $\{\eta_i\}=\{\eta^x_{A1},\eta^y_{A1},\eta^x_{A2},\eta^y_{A2}\}$, $m=1,2,3$. As it is easy to show [35,36], the lowest symmetry phase corresponds to the maximal rank of the matrix $(\mathrm{d}I_m/\mathrm{d}\eta_i)$ and consequently to $(\mathrm{d}F_{\mathrm{hom}}/\mathrm{d}I_m)=0$. Other ordered phases correspond to the different degenerations of the matrix: $(\mathrm{d}I_m/\mathrm{d}\eta_i)=0$. In the parent S_A phase all the components of the OP are equal to zero together with the rank of $(\mathrm{d}I_m/\mathrm{d}\eta_i)$. Using this method, we obtain *five different four-layer antiferroelectric phases*, characterized by the following relations between the $\boldsymbol{\eta}_{A1}$ and $\boldsymbol{\eta}_{A2}$ vectors (and consequently between the axial vectors $\boldsymbol{\eta}_1,\boldsymbol{\eta}_2,\boldsymbol{\eta}_3,\boldsymbol{\eta}_4$ of the tilts of four successive layers):

$$\left.\begin{array}{ll}
\mathbf{I}. & (\eta_{A1})^2=(\eta_{A2})^2 \text{ and } \boldsymbol{\eta}_{A1}\perp\boldsymbol{\eta}_{A2} \\
 & (\boldsymbol{\eta}_i,\boldsymbol{\eta}_{i+1})=\pi/2 \\
 & \qquad\text{or} \\
 & (\eta_i)^2=(\eta_m)^2 \text{ and } \boldsymbol{\eta}_i\perp\boldsymbol{\eta}_{i+1} \\
\mathbf{I}'. & (\eta_{A1})^2=(\eta_{A2})^2 \text{ and } \boldsymbol{\eta}_{A1}\perp\boldsymbol{\eta}_{A2} \\
 & (\boldsymbol{\eta}_i,\boldsymbol{\eta}_{i+1})=-\pi/2 \\
 & \qquad\text{or} \\
 & (\eta_i)^2=(\eta_m)^2 \text{ and } \boldsymbol{\eta}_i\perp\boldsymbol{\eta}_{i+1} \\
\mathbf{II}. & (\eta_{A1})^2=(\eta_{A2})^2 \\
 & \qquad\text{or} \\
 & (\eta_i)^2\neq(\eta_m)^2 \text{ and } \boldsymbol{\eta}_i\perp\boldsymbol{\eta}_{i+1} \\
\mathbf{VI}. & \boldsymbol{\eta}_{A1}\perp\boldsymbol{\eta}_{A2} \\
 & \qquad\text{or} \\
 & (\eta_i)^2=(\eta_m)^2 \\
\mathbf{IV}. & \text{no relation between } \boldsymbol{\eta}_{A1} \text{ and } \boldsymbol{\eta}_{A2}.
\end{array}\right\} \tag{6}$$

Corresponding structures are shown in figure 2. The axial vectors of the tilts in the four layers are presented and their projections on the (x,y)-plane.

It is evident that the absence of mirror planes in the chiral S_A^* phase and the existence in the free energy of the Dzyaloshinskii invariant $I_3=[\boldsymbol{\eta}_{A1}\times\boldsymbol{\eta}_{A2}]$ *do not permit the existence of four-layer phases with the molecules lying in the same plane.* Between the four-layer antiferroelectric smectic phases listed in (6), the structures noted as **I** and **I′** have the same symmetry, but in the phase **I′**, four vectors of the tilts form a right spiral, whereas in phase **I** they form a left spiral. The free energies of these phases are quite different, because of the different signs of the Dzyaloshinskii invariant I_3, which correspond to the left and to the right handed four-layer spirals. Usually phases of this type are called anti-isostructural [31,37,38].

From the thermodynamical point of view [39], the phases **I** and **I′** are the most probable to be found experimentally from amongst the five listed four-layer phases, because there is *only one component of the OP varying with temperature in these phases.* They can be described by the simplest Landau–de Gennes free energy expansion of the fourth degree. Eventual observation of the phases **II–IV** needs a high non-linearity of the system, which is expressed theoretically by higher order terms in the free energy. Note, that free energy expansion up to the eighth degree gives, in the case of four-layer ordering, regions of stability of all the listed phases.

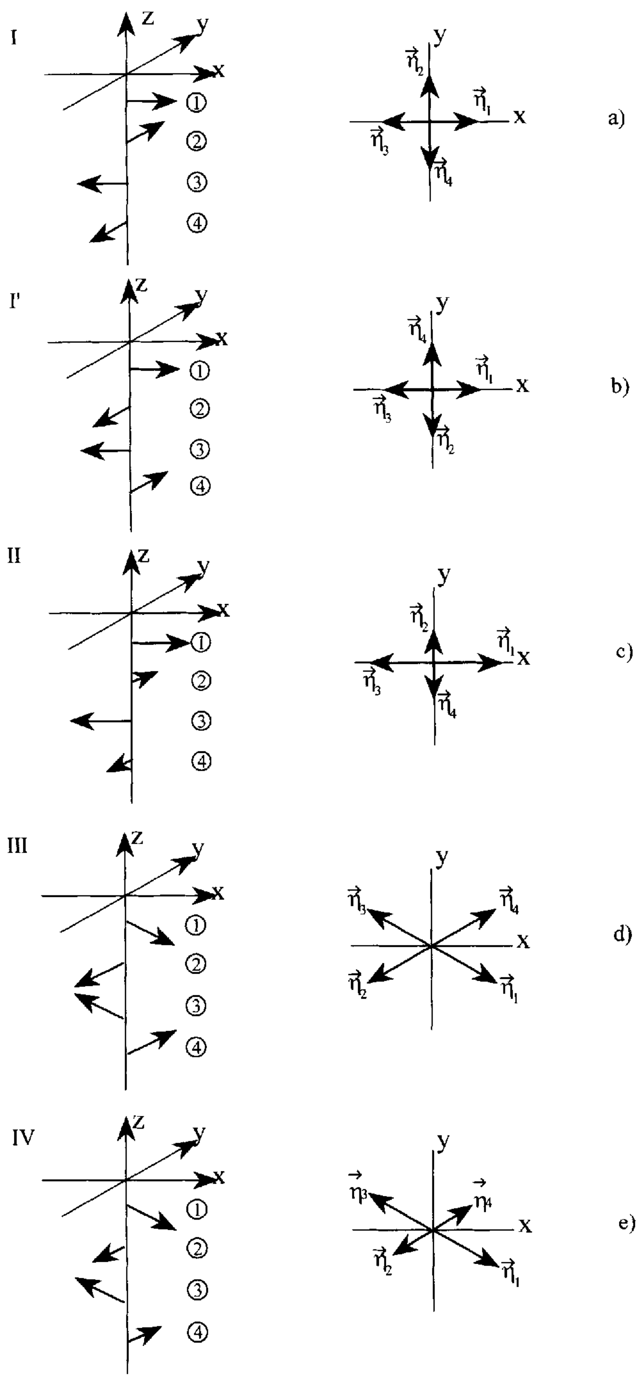

Figure 2. Structures of the different four-layer antiferroelectric phases. The vectors of the tilts in four successive layers are presented and their projection onto the smectic plane. The description of the phases is given by equation (6). (*a*) phase **I**; (*b*) phase **I′**; (*c*) phase **II**; (*d*) phase **III**; (*e*) phase **IV**.

One can generalize the description given for $n=4$ to the case of any even value of n. Actually, for any even n, the phase transition will be described by two vectors η_{A1} and η_{A2}. But for n layers, the axial vectors η_{A1} and η_{A2} are the symmetric combinations of the tilts of n layers and not four layers. However, for any n there will always be five antiferroelectric phases, described by the same relations between η_{A1} and η_{A2} as in equations (6) (the relation between η_i and η_{i+1} being, of course, different and dependent on the value of n). In the case of odd values of n, the situation is almost the same. The main difference with respect to the case of even n consists in the appearance of the non-zero value of η_P induced as a secondary *OP* by the antiferroelectric *OP*. This is due to the non-trivial coupling which always exists between η_P and η_{A1} and η_{A2} in the case of odd n. Only the phases **I** and **I′** are truly antiferroelectric in this case. The phases **II**, **III** and **IV** are ferrielectric phases with improper polarization **P** induced by the coupling with the antiferroelectric *OP*.

Let us finally analyse what kind of structures can form Devil's staircases in multilayer tilted chiral smectics. As mentioned above, for any value of n, there are the most probable phases **I** and **I′** with one component of *OP* varying with temperature. They are represented by n-layer right- or left-handed spirals. Such a kind of structure exists also for irrational values of n, for which it represents an incommensurate structure of the spiral type. Using thermodynamic arguments again, one can also suppose that only one of two possible anti-isostructural spirals **I** and **I′** is realized for each given value of n, because the fixed sign of the Dzyaloshinskii interaction $I_3=[\eta_{A1}\times\eta_{A2}]$ favours a fixed sense of the spiral.

Thus, in multilayer chiral tilted smectics, the Devil's staircase can be understood as a *progressive azimuthal reorientation of the molecules in successive layers.* An antiferroelectric $S^*_{C_A}$ phase with two layers in the unit cell ($n=2$) can be taken as the first end point of the staircase (see figure 3 (*a*)). Due to the temperature dependence of the wave vector **k**, one obtains a number of intermediate structures, the spirals with $2<n<\infty$ (see figure 3 (*b*)), with the azimuthal angle between adjacent layers $\psi=2\pi/n$. The ferroelectric S^*_C phase is the second end point of this staircase. Actually, the S^*_C phase can be considered as the structure with an infinite number of layers in the unit cell ($n=\infty$), the corresponding azimuthal angle being $\psi=2\pi/\infty=0$ (see figure 3 (*c*)).

The present mechanism of the Devil's staircase is quite different from those proposed by Takezoe *et al.* [16], in which all the intermediate structures between S^*_C and $S^*_{C_A}$ are planar. However, as shown above and in [28], symmetry and thermodynamics arguments cannot favour planar structures in multilayer chiral smectics.

Let us also briefly discuss the probability of the existence of a Devil's staircase of any type in chiral smectic liquid crystals. For this aim we will consider the terms of the free energy responsible for the Devil's

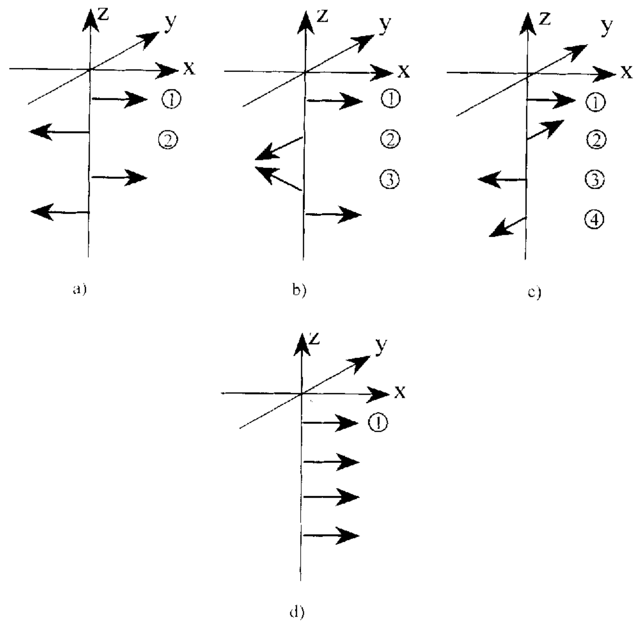

Figure 3. Possible types of Devil's staircase in multilayer chiral smectics. Temperature variation of the wave vector can be accompanied by progressive azimuthal reorientation of the molecules in successive layers. (*a*) $S^*_{C_A}$ phase as the first end point of the staircase; (*b*) and (*c*) intermediate structures; (*d*) S^*_C phase as the second end point of the staircase, the number of layers in the unit cell can be considered as infinite ($n = \infty$).

staircase and their dependence on the chirality of the system. There are usually two different types of term in the inhomogeneous part F_{inhom} of the Landau-de Gennes free energy—the terms of the Lifshitz-type, linearly dependent on gradients of the *OP*, and terms like the square of the gradient of the *OP*. The phenomenological coefficient multiplying the Lifshitz term can be considered as an 'inhomogeneous field'; it depends on the chirality of the system and becomes zero in the racemic mixture. By contrast, there is no evident reason for the coefficient multiplying the square of the gradient to be dependent on the composition of enantiomers. On the other hand, as it is well known [34, 38, 39] the existence of the temperature dependence of the wave vector **k** of the Devil's staircase type is connected with change in the sign of the latter coefficient. Thus, the Devil's staircase should not be strongly dependent on the concentration of enantiomers. However, as far as the author is aware, experiments performed on antiferroelectric liquid crystals show in all cases a rapid vanishing of the regions of stability of the intermediate phases with concentration, moving away from the optically pure substance (see, for example, [4]). Taking also into account the absence of clear-cut information about the structures of intermediate phases between S^*_C and $S^*_{C_A}$, one can conclude that for the moment there are no experimental data clearly speaking in favour of any Devil's staircase in chiral smectics.

3. Two isostructural helicoidal ferrielectric phases

Another interesting and unusual feature of multilayer phases with complex tilt and dipolar order is the possibility of existence of two isostructural ferrielectric phases. These phases have the same basic unwound structure, but their helicoidal structures are quite different; they differ in the value of the helical pitch and the sense of the helix.

To illustrate this possibility, let us generalize the two-layer model of the ferrielectric smectic phase previously developed by the authors [25, 26]. The main features of this model are in a good agreement with the results of dielectric and optical experiments performed on MHPOBC-type samples [4-(1-methylheptyloxycarbonyl)phenyl 4′-octyloxybiphenyl-4-carboxylate] and on series of liquid crystalline tolanes

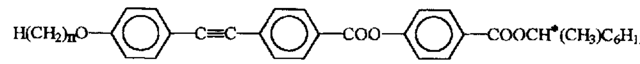

especially the temperatures dependences of the dielectric constant, of the relaxation frequencies and of the optical response [25, 26]. However one characteristic of this model was inconvenient. The corresponding Landau–de Gennes free energy of the inhomogeneous liquid crystal was restricted to the *fourth degree expansion* in the series of the *OP* components. Consequently, the phase transitions ferroelectric–ferrielectric and ferrielectric–antiferroelectric were described by the model as *second order*, in agreement with the group–sub-group relationship which exists between the structures of these phases. On the other hand, DSC measurements clearly show that the mentioned phase transitions are of the *first order*.

This situation is well known in the phenomenological theory of phase transitions. Usually, one can resolve this problem by including *terms of the sixth degree* in the free energy [31, 37–39]. Using this method we easily obtain the *sequence of first order phase transitions* S^*_C–$S^*_{C_\gamma}$–$S^*_{C_A}$ in the two-layer model. Furthermore, let us show that the *sixth-degree expansion of the Landau–de Gennes free energy in this case leads to the possibility of the existence of two isostructural helicoidal ferrielectric phases.* We introduce in the same way as in [25, 26] a two-component axial vector of the tilt $\boldsymbol{\eta}_i$, defined by equation (2), where $i = 1$ or 2. The four components of $\boldsymbol{\eta}_1$ and $\boldsymbol{\eta}_2$ of the tilts in two adjacent layers can be decomposed into symmetric and anti-symmetric combinations:

$$\boldsymbol{\eta}_P = \boldsymbol{\eta}_1 + \boldsymbol{\eta}_2 \quad \text{and} \quad \boldsymbol{\eta}_A = \boldsymbol{\eta}_1 - \boldsymbol{\eta}_2 \tag{7}$$

which span two irreducible representations of the space group of the S_A phase. Free energy expansion up to the sixth degree then contains the following terms:

$$F=(S/V)\int\left\{\frac{g_1}{2}\left(\frac{\partial\eta_P}{\partial z}\right)^2+\frac{g_2}{2}\left(\frac{\partial\eta_A}{\partial z}\right)^2\right.$$
$$+\lambda_1\left(\left(\frac{\partial\eta_{Px}}{\partial z}\right)\eta_{Py}-\left(\frac{\partial\eta_{Py}}{\partial z}\right)\eta_{Px}\right)$$
$$+\lambda_2\left(\left(\frac{\partial\eta_{Ax}}{\partial z}\right)\eta_{Ay}-\left(\frac{\partial\eta_{Ay}}{\partial z}\right)\eta_{Ax}\right)$$
$$+\frac{\alpha}{2}\eta_P^2+\frac{\beta}{4}\eta_P^4+\frac{a}{2}\eta_A^2+\frac{b}{4}\eta_A^4+\mathrm{d}\eta_P^2\eta_A^2$$
$$+\gamma(\boldsymbol{\eta}_P\boldsymbol{\eta}_A)^2+\frac{\delta}{3}\eta_P^6+\frac{c}{3}\eta_A^6+d_{13}\eta_P^2(\boldsymbol{\eta}_P\boldsymbol{\eta}_A)^2$$
$$\left.+d_{23}\eta_A^2(\boldsymbol{\eta}_P\boldsymbol{\eta}_A)^2+d_{112}\eta_P^4\eta_A^2+d_{122}\eta_P^2\eta_A^4\right\}\mathrm{d}z. \quad (8)$$

As the tilt angle in ferro-, ferri- and antiferroelectric phases remains nearly constant in all the layers [12, 13, 21], one can adopt for the following consideration the so called conical approximation, which permits the molecules in smectic layers to turn on cones, possessing *fixed vertex angles*. The tilt of each layer can be written than as: $\boldsymbol{\eta}_i=\eta_0(\cos\phi_i,\sin\phi_i)$, where η_0 is constant and ϕ_i is the azimuthal angle of the tilt axial vector of the ith layer. Using the in-phase and anti-phase azimuthal variables: $\phi=(\phi_i+\phi_{i+1})/2$; $\psi=(\phi_i-\phi_{i+1})/2$ one can express the OP in the form

$$\boldsymbol{\eta}_P=2\eta_0(\cos\phi\cos\psi,\sin\varphi\cos\psi);$$
$$\boldsymbol{\eta}_A=2\eta_0(-\sin\phi\sin\psi,\cos\phi\sin\psi). \quad (9)$$

Then, by substitution of the expression (9) into equation (8), the free energy can be rewritten as

$$F=(S/V)\int\left\{\frac{1}{2}\left(\frac{\partial\phi}{\partial z}\right)^2(g+\Delta g\cos 2\psi)\right.$$
$$+\frac{1}{2}\left(\frac{\partial\psi}{\partial z}\right)^2(g-\Delta g\cos 2\psi)$$
$$-\left(\frac{\partial\phi}{\partial z}\right)(\Lambda+\Delta\Lambda\cos 2\psi)+\frac{a_1}{2}\cos 2\psi$$
$$\left.+\frac{b_1}{4}\cos^2 2\psi+\frac{c_1}{6}\cos^3 2\psi\right\}\mathrm{d}z. \quad (10)$$

Note that the only difference in this free energy with respect to those proposed in [25, 26] is the last term in (10), which contains in conical approximation all the possible terms of the sixth degree.

Using Euler–Lagrange variational procedure, one can see that the stable solution corresponding to a helicoidal structure is described by $\phi=kz$; $\psi=C=f(z)$, where k is the wave vector characterizing the pitch of the helix, and C is the temperature dependent constant with respect to the space variables [25, 26]. For the ferroelectric helicoidal structure $\psi=0$, in the antiferroelectric helicoidal phase $\psi=\pi/2$ and ψ varies with temperature $(\pi/2>\psi(T)>0)$ in the intermediate ferrielectric phase.

Let us now focus our attention on the ferrielectric phase. The equations of state, which define the temperature dependence of the characteristics of this phase (see Appendix in [25]) are

$$k(g+\Delta g\cos 2\psi)-(\Lambda+\Delta\Lambda\cos 2\psi)=0;$$
$$2k\Delta\Lambda-k^2\Delta g-a_1-b_1\cos 2\psi-c_1\cos^2 2\psi=0. \quad (11)$$

Changing variables to the reduced symmetrized variables:

$$q=\Delta\Lambda-\Delta gk;$$
$$A=-a_1\Delta g+b_1g+(\Delta\Lambda)^2; \quad (12)$$
$$B=\Delta\Lambda g-\Delta g\Lambda$$

and excluding $\cos 2\psi$ from (11), we obtain the effective equation describing the ferrielectric phase:

$$q^4+q^2\left[-A+c_1\frac{g^2}{\Delta g}\right]+qB\left[b_1+2c_1\frac{g}{\Delta g}\right]+\frac{c_1}{\Delta g}B^2=0. \quad (13)$$

Here q is a reduced symmetrized wave vector of the helix, A and b_1 are temperature dependent phenomenological coefficients and B is the characteristic of effective chirality of the two-layer unit cell. This equation describes two different stable minima of the free energy of the two-layer ferrielectric state, which correspond to *two different isostructural helicoidal ferrielectric phases*. The schematic dependence of the free energy on the value of the wave vector q and on the value of $\cos 2\psi$ is presented in figure 4 (a). One can compare this dependence with those resulting from the fourth-degree expansion of the free energy (see equation (A8) in [25]) as shown in figure 4 (b).

Isostructural phase transition between two ferrielectric phases corresponds in the present model to vanishing of the coefficient multiplying the term linear in q in equation (13):

$$B\left[b_1+2c_1\frac{g}{\Delta g}\right]=0.$$

At the transition line, the reduced wave vector q undergoes a jump to its opposite value: $q_{FI}^{(2)}=-q_{FI}^{(1)}$. Thus, if the difference between the two Lifshitz coefficients $\Delta\Lambda=\lambda_1-\lambda_2$ is rather small (which is natural in a system with no difference between adjacent layers in the parent S_A phase), then the wave vector of the helix

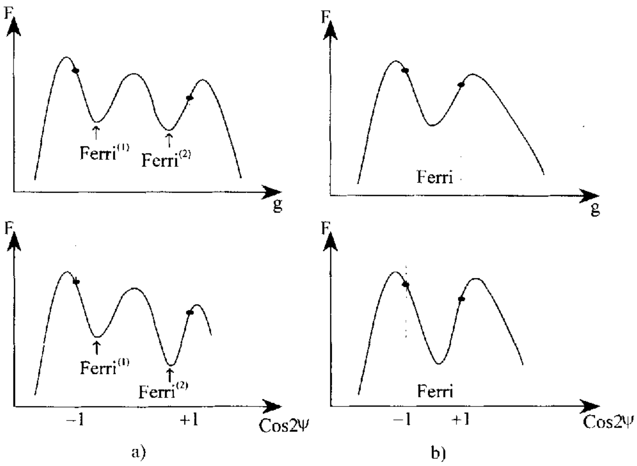

Figure 4. Schematic dependence of the free energy of the two-layer model of the ferrielectric phase on the value of the reduced wave vector q and on the value of $\cos 2\psi$, where ψ is an azimuthal angle between two adjacent layers. (*a*) Sixth-degree expansion; (*b*) fourth-degree expansion.

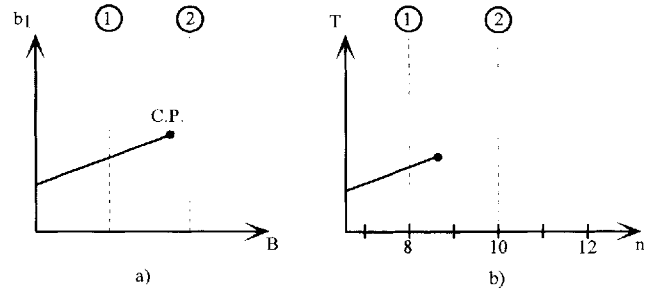

Figure 5. Schematic phase diagram presenting the line of isostructural phase transition which terminates in a critical point of the liquid–gas type. Two different thermodynamic paths are shown: path 1 intersects the line of transition between two ferrielectric phases; along path 2 the system does not undergo the transition. (*a*) phase diagram of the model (10); (*b*) eventual (temperature–chain length) phase diagram of the tolane family of liquid crystals.

k changes its sign at the Ferri$^{(1)}$–Ferri$^{(2)}$ transition (see the first equation in (12)). Consequently, two isostructural helicoidal ferrielectric phases should have different senses of their helices. If ΔA has a finite value, different from zero, the wave vector k has different absolute values in the two ferrielectric phases: $|k_{\mathrm{FI}}^{(2)}| \neq |k_{\mathrm{FI}}^{(1)}|$.

Summarizing the difference between and the common features of the Ferri$^{(1)}$ and Ferri$^{(2)}$ phases predicted by the model (10), we can note that, (i) *there is no qualitative difference between these two structures* possessing the same unwound basic structure. They are two-layer tilted structures with the same tilt angle in the layers and with the azimuthal angle between the layers different from zero and from π and (ii) there exist quantitative differences expressed by (*a*) *the difference of the pitch lengths* $p_{\mathrm{FI}}^{(1)} \neq p_{\mathrm{FI}}^{(2)}$, (*b*) *the different senses of the helices* $p_{\mathrm{FI}}^{(1)} > 0$; $p_{\mathrm{FI}}^{(2)} < 0$, (*c*) *the different average values of the azimuthal angle* $\psi_{\mathrm{FI}}^{(1)} \neq \psi_{\mathrm{FI}}^{(2)}$, and (*d*) *the different values of the free energy*.

The *difference in helical characteristics* should be clearly seen in *optical experiments*. The *difference in the free energies* should lead to a *DSC peak* at the Ferri$^{(1)}$–Ferri$^{(2)}$ transition and to *non-miscibility* of these phases.

It is necessary also to note that line of isostructural phase transitions can terminate in a *critical point of the liquid–gas type*. In a planar phase diagram of the model one can find, then, two types of thermodynamic path, which correspond to different regimes of evolution of the system (see figure 5(*a*)). First one intersects the transition line and the system undergoes a first order isostructural phase transition. The second path does not intersect the line and the system goes from one ferrielectric phase into another *without any transition at all*. This is possible because there is no qualitative difference between the phases. Schematic temperature dependences of the wave vector k and of the pitch of the helix corresponding to the two different thermodynamic paths are shown in figure 6. For the path intersecting the transition line, the pitch of the helix should undergo a finite jump with the change of the helix sense in the region of the ferroelectric $S_{C_\gamma}^*$ phase (see figure 6(*a*)), while along the second path, without any transition, the

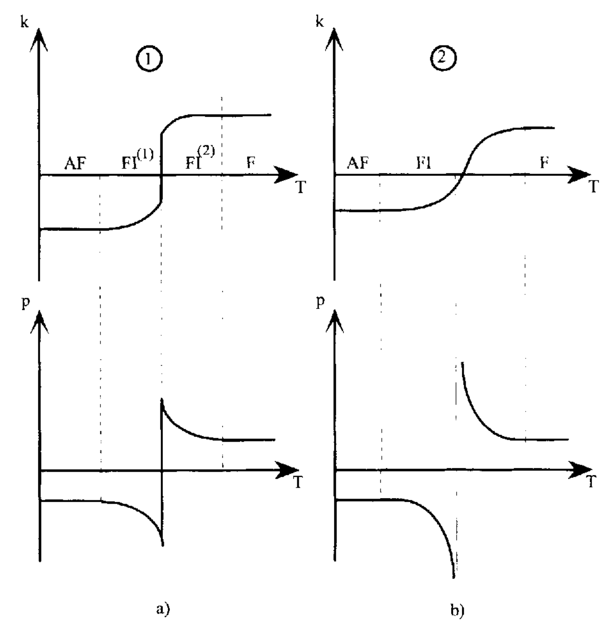

Figure 6. Schematic temperature dependences of the wave vector k and of the pitch p of the helix along two different thermodynamic paths in the phase diagram of figure 5. (*a*) path 1 with Ferri$^{(1)}$–Ferri$^{(2)}$ transition; (*b*) path 2 without phase transition.

wave vector k of the helix should change its sign continuously, which correspond to divergency of the pitch in a very narrow temperature region. The helix is unwound and then wound again in the opposite sense.

On experiment, the phase diagram 5(*a*) can correspond to the diagram (temperature–chain length) for the series of homologues of a liquid crystal family (see figure 5(*b*)). Actually, b_1 is temperature dependent and B depends only on the molecular characteristics of the substance. One can compare the predictions of the present model with recent results from DSC, miscibility and optical measurements performed on the family of tolane liquid crystal materials [21, 40, 41]. These materials show the existence of two non-miscible $S_{C_\gamma}^*$ phases for $n = 7$ and 8, although there is only one $S_{C_\gamma}^*$ phase in the sequence of phases for $n = 9$, 10, 11 and 12. The first order of the Ferri$^{(1)}$–Ferri$^{(2)}$ transition in the C7-tolane and the C8-tolane is confirmed by the well-resolved peak in the DSC measurements. The helical pitch measurements made by the Grandjean–Cano method and by selective band reflection show the inversion of the sense of the helix in the region of $S_{C_\gamma}^*$ phase. For $n = 10$ this change occurs approximately in the middle of $S_{C_\gamma}^*$ phase and is accompanied by a *rapid variation of the pitch value*, which can correspond to pitch divergence. In the case of $n = 8$, the *pitch undergoes a finite discontinuity* with change in sign exactly at the Ferri$^{(1)}$–Ferri$^{(2)}$ transition. These facts permit to suppose that the two $S_{C_\gamma}^*$ phases in the C7- and C8-tolanes are isostructural helicoidal ferrielectric phases. A possible (temperature-chain length) phase diagram of this family is schematized in figure 5(*b*). For $n = 9$, 10, 11 and 12, the thermodynamic path does not intersect the line of the isostructural phase transitions.

4. Discussion

This work illustrates only a part of new unusual features of multilayer smectic phases with complex tilt and dipolar order. Some other important characteristics of these phases could not be discussed here. These concern especially the macroscopic switching of defects due to thermal fluctuations in the ferrielectric phase and several complex inhomogeneous structures which can arise in these systems in an external electric field. Nevertheless, the points presented here: the multitude of multilayer antiferroelectric and ferrielectric phases and the possibility of isostructural helicoidal ferrielectric phases show in themselves the richness of this type of liquid crystal and the remarkable difference with respect to the classical ferroelectric S_C^* phase.

The author is grateful to Professor J. Prost and Drs J. Pavel and B. Mettout for stimulating discussions. The work was supported in part by the Region of Picardie.

References

[1] Chandani, A. D. L., Gorecka, E., Ouchi, Y., Takezoe, H., and Fukuda, A., 1989, *Jpn. J. appl. Phys.*, **28**, L1265.
[2] Chandani, A. D. L., Ouchi, Y., Takezoe, H., Fukuda, A., Terashima, K., Furukawa, K., and Kishi, A., 1989, *Jpn. J. appl. Phys.*, **28**, L1261.
[3] Fukuda, A., (editor), 1992, *Future Liquid Crystal Displays and its Materials* (Tokyo CMC).
[4] Fukuda, A., Takanishi, Y., Isozaki, T., Ishikawa, K., and Takezoe, H., 1994, *J. mater. Chem.*, **4**, 997.
[5] Fukui, M., Orihara, H., Yamada, Y., Yamamoto, N., and Ishibashi, Y., *Jpn. J. appl. Phys.*, **28**, L849.
[6] Gorecka, E., Chandani, A. D. L., Ouchi, Y., Takezoe, H., and Fukuda, A., 1990, *Jpn. J. appl. Phys.*, **29**, 131.
[7] Lee, J., Ouchi, Y., Takezoe, H., Fukuda, A., and Watanabe, J., 1990, *J. Phys. Cond. Matt.*, **2**, SA271.
[8] Takezoe, H., Lee, J., Chandani, A. D. L., Gorecka, E., Ouchi, Y., Fukuda, A., Terashima, K., and Furukava, K., 1991, *Ferroelectrics*, **114**, 187.
[9] Levelut, A. M., Germain, C., Keller, P., Liebert, L., and Billard, J., 1983, *J. Phys. (France)*, **44**, 623.
[10] Beresnev, L. A., Blinov, L., Osipov, M. A., and Pikin, S. A., 1988, *Molec. Cryst. liq. Cryst.*, **158A**, 3.
[11] Galerne, Y., and Liebert, L., 1989, *Abstract of 2nd Int. Symp. on FLCs, (Göteborg)*, O27.
[12] Levelut, A. M., and Gisse, P., 1992, private communication.
[13] Suzuki, A., Orihara, H., Ishibashi, Y., Yamada, Y., Yamamoto, N., Mori, K., Nakamura, K., Suzuki, Y., Hagiwara, T., Kawamura, Y., and Fukuwi, M., 1990, *Jpn. J. appl. Phys.*, **29**, L336.
[14] Inui, S., Kawano, S., Saito, M., Iwane, H., Takanishi, Y., Hiraoka, K., Ouchi, Y., Takezoe, H., and Fukuda, A., 1990, *Jpn. J. appl. Phys.*, **29**, L987.
[15] Goodby, J. W., Patel, J. S., and Chin, E., 1992, *J. mater. Chem.*, **2**, 197.
[16] Takezoe, H., Lee, J., Ouchi, Y., and Fukuda, A., 1991, *Molec. Cryst. liq. Cryst.*, **202**, 85.
[17] Musevic, I., Blinc, R., Zeks, B., Copic, M., Witterbrood, M. M., Rasing, T. H., Orihara, H., and Ishibashi, Y., 1993, *Phys. Rev. Lett.*, **1**, 1180.
[18] Isozaki, T., Fujikawa, T., Takezoe, H., Fukuda, A., Hagiwara, T., Suzuki, Y., and Kawamura, I., 1993, *Phys. Rev. B*, **48**, 13439.
[19] Fujikawa, T., Hiraoka, K., Isozaki, T., Kagikawa, K., Takezoe, H., and Fukuda, A., 1993, *Jpn. J. appl. Phys.*, **32**, 985.
[20] Johno, M., Ouchi, Y., Takezoe, H., and Fukuda, A., 1990, *Jpn. J. appl. Phys.*, **29**, L111.
[21] Cluzeau, P., Nguyen, H. T., Destrade, C., Isaert, N., Barois, P., and Babeau, A. (to be published).
[22] Orihara, H., and Ishibashi, Y., 1990, *Jpn. J. appl. Phys.*, **29**, L115.
[23] Zeks, B., Blinc, R., and Cepic, M., 1991, *Ferroelectrics*, **122**, 221.
[24] Zeks, B., and Cepic, M., 1993, *Liq. Cryst.*, **14**, 445.
[25] Lorman, V. L., Bulbitch, A. A., and Toledano, P., 1994, *Phys. Rev. E*, **49**, 1367.
[26] Gisse, P., Pavel, J., Nguyen, H. T., and Lorman, V. L., 1993, *Ferroelectrics*, **147**, 27.
[27] Isozaki, T., Fujikawa, T., Takezoe, H., Fukuda, A., Hagiwara, T., Suzuki, Y., and Kawamura, I., 1992, *Jpn. J. appl. Phys.*, **31**, L1435.

[28] (a) LORMAN, V. L., *Molec. Cryst. liq. Cryst.*, to be published in *Mol. Cryst. Liq. Cryst.*; (b) LORMAN, V. L., 1994, 15th International Liquid Crystal Conference, 3–8 July, Budapest, to be published in *Mol. Cryst. Liq. Cryst.*
[29] INDENBOM, V. L., PIKIN, S. A., and LOGINOV, E. B., 1976, *Soviet Phys. Crystallogr.*, **21,** 632.
[30] INDENBOM, V. L., and LOGINOV, E. B., 1981, *Soviet Phys. Crystallogr.*, **26,** 526.
[31] TOLEDANO, J. C., and TOLEDANO, P., 1987, *The Landau Theory of Phase Transitions* (Singapore: World Scientific).
[32] DZYALOSHINSKII, I. E., 1964, *JETP*, **46,** 1352.
[33] BAK, P., 1982, *Rep. Prog. Phys.*, **45,** 587.
[34] DZYALOSHINSKII, I. E., 1964, *JETP*, **47,** 992.
[35] GUFAN, YU. M., KUTYIN, E. I., LORMAN, V. L., PROKHOROV, A. M., and RUDASHEVSKII, E. G., 1987, *JETP Lett.*, **46,** 287.
[36] KUTYIN, E. I., LORMAN, V. L., and PAVLOV, S. V., 1991, *Sov. Phys. Usp.*, **34,** 497.
[37] GUFAN, YU. M., 1982, *Structural Phase Transitions* (Moscow: Nauka).
[38] IZYUMOV, YU. A., and SYROMIATNIKOV, V. N., 1984, *Phase Transitions and Symmetry of Crystals* (Moscow: Nauka).
[39] LANDAU, L. D., and LIFSHITZ, E. M., 1969, *Statistical Physics* (Oxford: Pergamon Press).
[40] DESTRADE, C., CLUZEAU, P., BAROIS, P., ISAERT, N., ROUILLON, J. C., and NGUYEN, H. T., 1994, 15th International Liquid Crystal Conference, 3–8 July, Budapest, to be published in *Mol. Cryst. Liq. Cryst.*
[41] GISSE, P., SIDIR, M., PAVEL, J., LORMAN, V. L., FARHI, R., and NGUYEN, H. T., 1994, 15th International Liquid Crystal Conference, 3–8 July, Budapest, to be published in *Mol. Cryst. Liq. Cryst.*